DOI:10.22337/2587-9618-2026-22-3-175-188

# EVALUATION OF THE BUCKLING OF FRAME STRUCTURES UNDER DYNAMIC LOADING, TAKING INTO ACCOUNT THE INERTIAL COMPONENTS OF INTERNAL FORCES

***Vladimir N. Sidorov*, *Vadim K. Akhmetov, Dmitriy O. Klimushkin***
National Research Moscow State University of Civil Engineering, Moscow, RUSSIA

**Abstract:** An approach to directly assessing the stability of a flat frame structure under unsteady dynamic loading is proposed and numerically investigated. In contrast to the traditional choice of a single static or quasi-static calculation case, at each step of integrating the equation of motion, an instantaneous stability problem is formed, taking into account the inertial components on the left-hand side of the operator equation and in the local forces that determine the geometric rigidity of the calculation model. The contribution of longitudinal and transverse forces, as well as nodal bending moments in resisting the loss of stability of beam elements of the Timoshenko model, is considered together. The method is implemented in the author's finite element program in Python and compared with the nonlinear quasi-static calculation in the Simulia Abaqus/Standard PC environment using the Riks method (Static, Riks). The buckling resistance of the load-bearing frame structure of an industrial building was studied. Its finite element model includes 246 nodes and 369 finite elements. The equation of motion is solved in the time interval 0 – 129.99 sec with a step of 0.01 sec. Analysis of the entire time history showed the presence of single spectral emissions; after checking the temporal stability of the eigenvalues, the physical minimum of the stability margin factor $\Lambda_{min}$ (SMF) was established at step 7913 (time $t$ = 79.13 s, $\Lambda_{min}$ = 25.10992). Additionally, the multimode event at step 4138 and time slices selected based on the maximum displacements of nodes in hazardous areas are considered. For two slices generated using the same exact method, SIMULIA Abaqus confirmed the same ranking: the critical value of the load proportionality factor (LPF) obtained using the Ricks method is 48.21736 for $t$ = 41.38 s and 44.42943 for $t$ = 79.13 s. It is shown that the absolute values of the direct SMF and LPF are not identical due to the difference in the formulations of the problem being solved, but the consistency of the dangerous moment in time confirms the diagnostic value of the proposed method.

**Keywords:** dynamic stability; frame structure; finite element method; Timoshenko beam; inertial forces; geometric stiffness; stability margin; SIMULIA Abaqus; Riks method

# ОЦЕНКА УСТОЙЧИВОСТИ РАМНЫХ КОНСТРУКЦИЙ ПРИ ИХ ДИНАМИЧЕСКОМ НАГРУЖЕНИИ С УЧЁТОМ ИНЕРЦИОННЫХ СОСТАВЛЯЮЩИХ ВНУТРЕННИХ УСИЛИЙ

***В.Н. Сидоров*, *В.К. Ахметов*, *Д.О. Климушкин***
Национальный исследовательский Московский государственный строительный университет, г. Москва, РОССИЯ

**Аннотация.** Предложен и численно исследован подход к прямой оценке устойчивости плоской рамной конструкции в процессе нестационарного динамического нагружения. В отличие от традиционного выбора одного статического или квазистатического расчётного случая, на каждом шаге интегрирования уравнения движения формируется мгновенная задача устойчивости, учитывающая инерционные компоненты в левой части операторного уравнения и в локальных усилиях, определяющих геометрическую жёсткость расчетной модели. Вклад продольных и поперечных сил, а также узловых изгибающих моментов при сопротивлении потере устойчивости балочных элементов модели Тимошенко рассматривается совместно. Метод реализован в авторской конечно-элементной программе на Python и сопоставлен с нелинейным квазистатическим расчётом в среде ПК SIMULIA Abaqus/Standard методом

Рикса (Static, Riks). Исследовано сопротивление потере устойчивости несущей рамной конструкции промышленного здания. Ее расчетная конечно-элементная модель включает 246 узлов и 369 стержневых элементов. Уравнение движения решается во временном интервале 0 – 129,99 сек с шагом 0,01 сек. Анализ всей временной истории показал наличие одиночных спектральных выбросов; после контроля временной устойчивости собственных значений физический минимум коэффициента запаса устойчивости $\Lambda_{min}$ (КЗУ (SMF)) установлен на шаге 7913 (момент времени $t$ = 79,13 с, $\Lambda_{min}$ = 25,10992). Дополнительно рассмотрено многомодовое событие на шаге 4138 и временные срезы, выбранные по максимумам перемещений узлов в опасных зонах. Для двух срезов, сформированных единым точным способом, SIMULIA Abaqus подтвердил одинаковое ранжирование: полученное методом Рикса критическое значение коэффициента пропорциональности нагрузки (LPF) равен 48,21736 для $t$ = 41,38 с и 44,42943 для $t$ = 79,13 с. Показано, что абсолютные значения прямого КЗУ и LPF не являются тождественными вследствие различия постановок решаемой задачи, однако согласованность опасного момента времени подтверждает диагностическую ценность предложенной методики.

**Ключевые слова:** динамическая устойчивость; рамная конструкция; метод конечных элементов; балка Тимошенко; инерционные силы; геометрическая жёсткость; коэффициент запаса устойчивости; SIMULIA Abaqus; метод Рикса

## INTRODUCTION

The development of the finite element method (FEM) transformed the analysis of complex mechanical systems from a collection of particular analytical problems into a general computational procedure. Following the work of R. Clough, which established the term finite element method [1], variational and matrix formulations of the FEM were developed systematically [2, 3]. In stability analysis, this enabled a transition from individual formulae for assessing the stability of a member with an effective length or of a frame to an eigenvalue problem based on global elastic and geometric stiffness matrices.

Two principal static approaches are used in engineering practice. The first, linear bifurcation analysis, determines eigenvalue load multipliers for an idealised prestressed state. The second, nonlinear analysis, traces the equilibrium path with allowance for large displacements, initial imperfections and, where necessary, material nonlinearity [4]. The latter approach underlies the limit-state design procedures specified in Eurocode 3 [5] and SP 16.13330 [6]. The choice of the initial loading remains essential: a static loading scheme contains no information about the distribution of inertia forces at a particular instant of the system's motion.

Dynamic stability is a broader problem. Classical theory addresses parametric excitation, instability regions and the behaviour of systems with varying coefficients in their differential equations [7]. General criteria for the stability of motion originate in the work of A. M. Lyapunov [8] and the development of energy methods for deformable systems [9]. Modern theories emphasise the distinction between the stability of equilibrium and the stability of motion [10]. In civil engineering structures, this problem arises under wind and aeroelastic actions [11], earthquakes, and impulsive or suddenly applied loads [12].

Commercial finite-element packages provide direct dynamic analysis and, separately, linear or nonlinear stability analysis. However, an algorithmic stability assessment of every instantaneous state along the dynamic time history is generally unavailable. The engineer must therefore select one or more instants in advance, transfer the displacements or equivalent forces to a static model, and then perform a quasi-static analysis. Selecting the instant of maximum displacement of an individual node is convenient, but does not guarantee that it coincides with the minimum overall stability margin of the structure.

The choice of beam-element kinematics also affects the result. Euler–Bernoulli theory neglects shear deformation, whereas S. P. Timoshenko's model accounts for independent cross-section rotation and transverse shear [13]. In dynamic analysis, the representation of elastic

stiffness and inertia forces is important, as is the dissipation model. References [14, 15] proposed matrix forms of internal damping for rod elements consistent with an energy-based formulation.

The foundations of the instantaneous stability problem implemented in this study were formulated in [16, 17, 18]. The authors previously developed the inclusion of contributions from axial forces, bending moments and shear forces in the geometric stiffness of rod systems [19]. Earlier publications associated with the present research described the algorithm and model parameters, but did not include numerical modelling of the time history or a comparison of critical states. The aim of this work is to assess whether the direct dynamic stability margin factor can identify unfavourable instants confirmed by an independent nonlinear quasi-static analysis in Abaqus/Standard [20].

The scientific novelty of the study consists in jointly considering: (1) the inertia operator on the left-hand side of the instantaneous eigenvalue problem; (2) the dynamic components of local internal forces used to define the geometric stiffness of the computational model; (3) the complete set of internal-force components N–Q–M of a rod element in stability analysis; (4) the temporal persistence of the spectrum and rejection of isolated eigenvalues; and (5) comparison of the selected critical instants with Riks-method results obtained for the same spatial distribution of dynamic forces.

## 1. FORMULATION OF THE DIRECT DYNAMIC STABILITY PROBLEM

The motion of the discrete finite-element system is described by the matrix form of d'Alembert's equation:

$$\mathbf{M}\cdot\ddot{\bar{\mathbf{V}}}(t)+\mathbf{D}\cdot\dot{\bar{\mathbf{V}}}(t)+\mathbf{K}\cdot\bar{\mathbf{V}}(t)=\bar{\boldsymbol{F}}(t), \quad (1)$$

where **M**, **D** and **K** are the global mass, damping and elastic stiffness matrices of the computational model; $\bar{\mathbf{V}}$ , $\dot{\bar{\mathbf{V}}}$ and $\ddot{\bar{\mathbf{V}}}$ are the displacement, velocity and acceleration vectors; and $\bar{\boldsymbol{F}}$(t) is the external load vector prescribed as a function of time *t*.

To represent the dynamic contributions, diagonal coefficient matrices are introduced that relate the inertia and dissipative forces to the elastic forces at the corresponding global degrees of freedom:

$$\mathbf{A}_{in}=diag((\mathbf{M}\cdot\ddot{\bar{\mathbf{V}}})_{[i]}:(\mathbf{K}\cdot\bar{\mathbf{V}})_{[i]})=diag((\bar{\mathbf{S}}_{in})_{[i]}:(\bar{\mathbf{S}}_{el})_{[i]}), \quad (2)$$

$$\mathbf{A}_{damp}=diag((\mathbf{D}\cdot\dot{\bar{\mathbf{V}}})_{[i]}:(\mathbf{K}\cdot\bar{\mathbf{V}})_{[i]})=diag((\bar{\mathbf{S}}_{damp})_{[i]}:(\bar{\mathbf{S}}_{el})_{[i]}), \quad (3)$$

The ratios of inertia forces to elastic forces are evaluated only when the denominator is sufficiently large and are subjected to regularisation. This prevents division by near-zero components, but does not replace the subsequent verification of the temporal persistence of the eigenvalue spectrum.

The equation of motion can thus be rewritten in operator form:

$$(\mathbf{A}_{din}+\mathbf{E})\cdot\mathbf{K}\cdot\bar{\mathbf{V}}(t)=\bar{\boldsymbol{F}}(t). \quad (4)$$

where $\mathbf{A}_{din} = \mathbf{A}_{in} + \mathbf{A}_{damp}$, and **E** is the identity matrix. The stability formulation adopts the hypothesis that dissipative forces do not produce a potential contribution that directly changes the critical state [17]. Accordingly, only the inertia operator $\mathbf{A}_{in}$ is retained on the left-hand side of the eigenvalue problem.

The instantaneous stability problem at time t is written as:

$$(\mathbf{A}_{din}+\mathbf{E})\cdot\mathbf{K}\cdot\Phi=\mathbf{K}^{\Gamma}\cdot\Phi\cdot\boldsymbol{\Lambda}, \quad (5)$$

Here $\boldsymbol{\Lambda}$ is the diagonal matrix of stability margin factors, and the columns of Φ describe the corresponding buckling modes. The smallest positive real value $\boldsymbol{\Lambda}_{\min}(t)$ is treated as the

minimum instantaneous stability margin factor of the structure.

The complete geometric stiffness matrix of the computational model is assembled as the sum:

$$\mathbf{K}^{\Gamma} = \mathbf{K}_N^{\Gamma} + \mathbf{K}_M^{\Gamma} + \mathbf{K}_Q^{\Gamma}. \qquad (6)$$

where $\mathbf{K}_N^{\Gamma}$ is the conventional contribution of axial forces, $\mathbf{K}_M^{\Gamma}$ is the contribution of nodal bending moments, and $\mathbf{K}_Q^{\Gamma}$ is the contribution of shear forces. The local internal-force vector of a two-node planar rod element has the form [$N_1$, $Q_1$, $M_1$, $N_2$, $Q_2$, $M_2$]. Only the elastic and inertial contributions are included when forming the dynamic internal forces.

Thus, inertia forces are accounted for both on the left-hand side of (5) and in the internal forces that determine the geometric stiffness matrix $\mathbf{K}^{\Gamma}$ on the right-hand side of the eigenvalue problem. This distinguishes the direct dynamic factor from the proportionality factor of a frozen static load. Figure 1 summarises the comparison procedure.

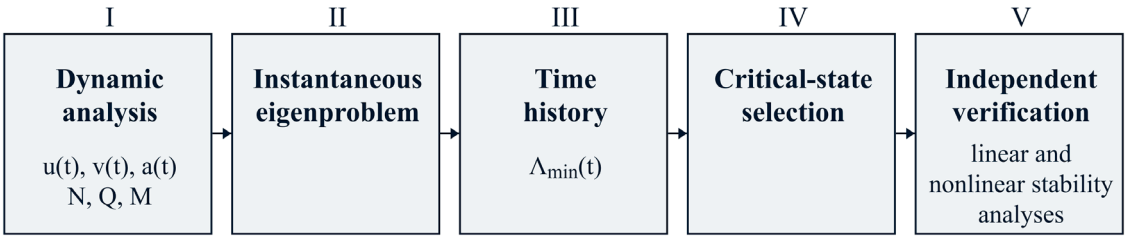



*Figure 1. Sequence used to compare the direct dynamic and quasi-static results*

## 2. COMPUTATIONAL MODEL AND NUMERICAL IMPLEMENTATION

### *2.1. Geometry, Finite Elements, and Material Properties*

The stability of a load-bearing planar steel frame of an industrial building was investigated. The frame comprises columns, beams, truss chords and internal working platforms. Its overall dimensions along the coordinate axes are 47.70 × 27.41 m. The finite-element computational model contains 246 nodes and 369 two-node rod elements, with three degrees of freedom per node. Before constraints are applied, the system has 738 degrees of freedom; boundary conditions constrain 27 degrees of freedom at nine nodes. The computational model and control nodes are shown in Figure 2.

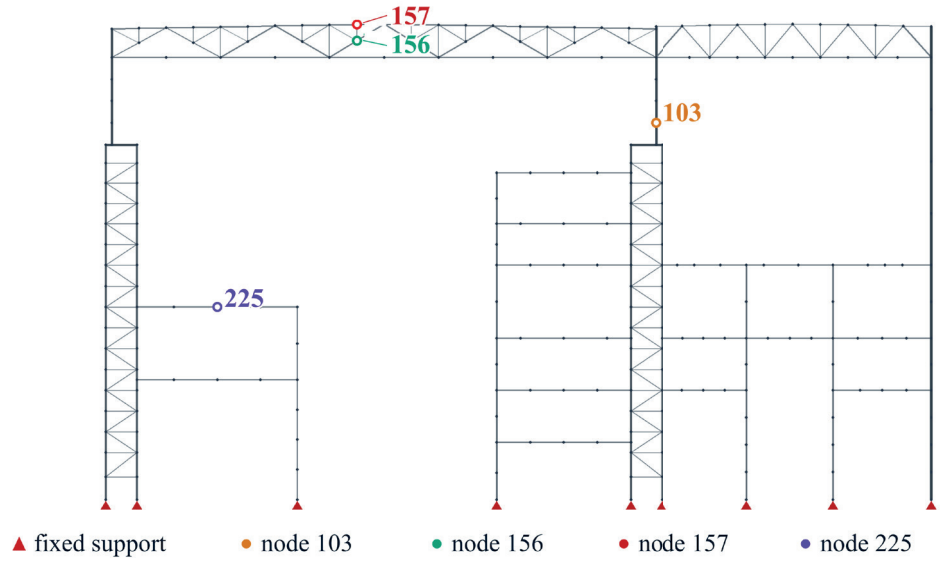



*Figure 2. Finite-element model of the investigated frame and control nodes*

Inspection of the local element stiffness matrices identified 13 short elements for which the shear contribution resulted in a non-positive-definite local stiffness matrix. Twelve elements were treated using the Euler–Bernoulli model without changing their geometry. One element, 5 mm long, was replaced by a rigid kinematic link between neighbouring nodes. This regularisation preserves the global topology and eliminates artificial local mechanisms.

*Table 1. Main parameters of the computational model*

| Parameter | Adopted value |
|---|---|
| Model size | 246 nodes; 369 elements; 738 nodal degrees of freedom |
| Overall dimensions | X: −0.05 to 47.65 m; Y: 0 to 27.41 m |
| Material | E = 210 GPa; $\rho$ = 7850 kg/m³; $\nu$ = 0.30; reference yield stress 350 MPa |
| Cross-sections | 15 types; A = 2.12 × $10^{-3}$ to 5.91 × $10^{-2}$ m²; I = 2.20 × $10^{-5}$ to 1.082 × $10^{-2}$ m⁴ |
| Time grid | $\Delta t$ = 0.01 s; 13,000 samples; analysis interval 0–129.99 s |
| Damping | Rayleigh damping ratio $\zeta$ = 0.05; calibration against eigenmodes 1 and 111 |
| Stability model | Timoshenko elements; deformed-configuration analysis; N, Q, and M included in the stability equation |
| Loads | 167 components: 130 constant, 28 harmonic, and 9 piecewise-linear |
| Spectral control | Regularization of ill-conditioned systems; symmetric seven-step temporal window |

### *2.2. Loading and Time Integration of The Equations of Motion*

The loading history comprises 167 active components: 92 concentrated and 75 distributed loads. Their time dependence consists of 130 constant, 14 sinusoidal, 14 cosinusoidal and nine piecewise-linear components. Of these, 137 act vertically and 30 horizontally. This time-dependent representation reproduces the combined action of constant operational loads, harmonic actions and transient equipment operating regimes. Representative piecewise-linear load histories applied to the frame are shown in Figure 3.

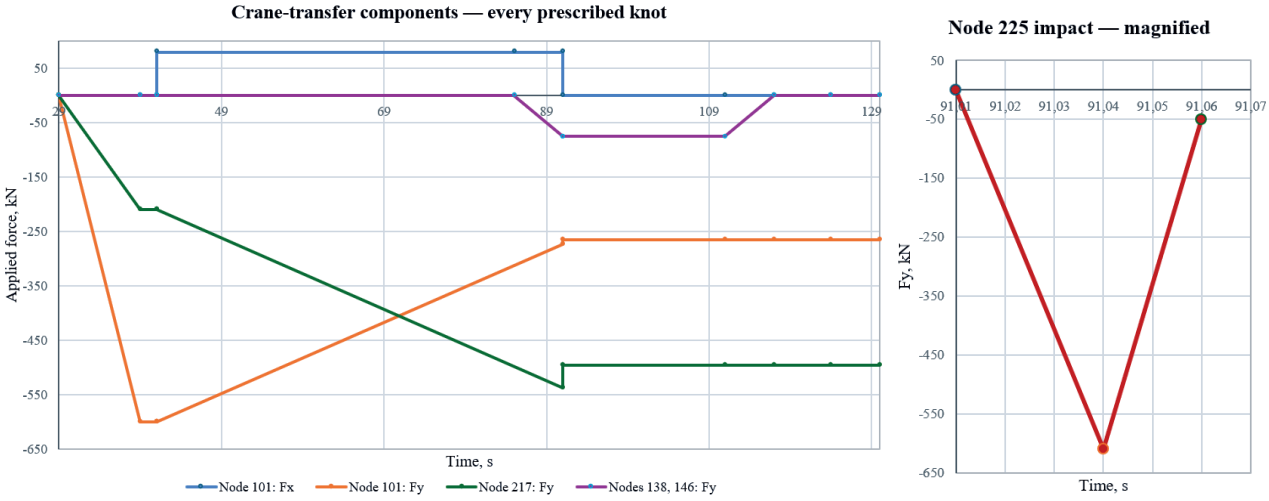



*Figure 3. Representative piecewise-linear load histories applied to the frame*

Equation (1) is integrated using the Newmark method with a time step of 0.01 s. At each step, a system of linear equations is solved with the following effective coefficient matrix:

$$\mathbf{Z}=\frac{2}{\Delta t^2}\cdot\mathbf{M}+\frac{1}{\Delta t}\cdot\mathbf{D}+\mathbf{K} \quad (7)$$

The acceleration and velocity are then recovered recursively. During direct integration, the nodal coordinates of the computational model are also updated at the new step using the displacements from the previous step. The stiffness, mass and damping matrices are recalculated for the current geometry. The damping coefficients are determined at the first time step and subsequently remain constant.

### *2.3. Processing of the Stability Spectrum*

The eigenvalues are determined for the instantaneous combination of elastic and geometric stiffness. A regularised solution is used when conditioning deteriorates. The final spectrum retains positive, nearly real values associated with physical buckling modes; auxiliary roots are excluded.

A temporal criterion is used to exclude isolated spectral rearrangements: a sequence of neighbouring values and the continuity of the corresponding eigenmodes are examined. The start-up interval is excluded, and the minimum-factor series is additionally processed using a symmetric seven-step window. A physical minimum is identified as a decrease along the same spectral branch that persists over a time interval.

## 3. QUASI-STATIC ANALYSIS IN SIMULIA ABAQUS

The calculation was performed in Abaqus/Standard using a model assembled from B31 beam elements. An implicit dynamic analysis of the structure is first carried out, and the resulting nodal displacements U, accelerations A and resultant nodal forces are extracted over the prescribed full time interval.

The stability investigation comprised three levels: linear modal analysis, direct implicit dynamic analysis and geometrically nonlinear stability analysis using the Riks method (arc-length method). This combination allows the agreement of mass–stiffness characteristics, dynamic response and limit states to be assessed separately.

The Riks method is an arc-length continuation method for nonlinear equilibrium analysis in the vicinity of a bifurcation. At each increment, the displacement vector and the load multiplier are updated simultaneously, while an additional arc-length constraint defines the step length in load–displacement space. This permits the solution to pass a limit point and trace a descending equilibrium branch, where conventional load control becomes unstable [20, 21].

The maximum load multiplier at the limit point is adopted as the critical result. For the states at $t$ = 41.38 s and $t$ = 79.13 s, the force distributions and deformed geometry were transferred using the same synchronised procedure and used for quantitative comparison. States selected from the displacement maxima of individual nodes were considered additional control cases.

Five states of the dynamic process were used for nonlinear verification: $t$ = 41.38, 41.62, 41.65, 79.13 and 124.04 s. The first and fourth were selected from characteristic values of the global stability factor; the others were selected from displacement maxima at the control nodes. In each case, the static model reproduces the force distribution of the corresponding dynamic state.

The comparison considers the time at which an unfavourable state occurs, the relative ranking of the cases, the critical multiplier and the buckling-mode characteristics. Absolute agreement between the factors is not required, because the direct dynamic and nonlinear quasi-static formulations use different operators.

## 4. RESULTS

### *4.1. Minimum Stability Factor Over the Complete Time History*

Linear verification was performed by comparing the first ten natural frequencies (Table 2). The mean absolute deviation of the in-house model from Abaqus was 2.87%, and

the maximum deviation was 8.96%. For the first six modes, which are most significant in the dynamic-response range considered, the mean deviation was 1.48%. This confirms the agreement of the global mass and stiffness matrices of the two models.

*Table 2. Comparison of the natural frequencies*

| Mode | In-house model, Hz | Abaqus, Hz | Difference, % |
|---|---|---|---|
| 1 | 0.5931 | 0.5911 | 0.34 |
| 2 | 0.8211 | 0.8265 | 0.66 |
| 3 | 1.1694 | 1.1743 | 0.42 |
| 4 | 1.4475 | 1.4675 | 1.36 |
| 5 | 1.7356 | 1.7630 | 1.55 |
| 6 | 1.9389 | 1.9831 | 2.23 |
| 7 | 2.0621 | 2.1880 | 5.75 |
| 8 | 2.3922 | 2.6275 | 8.96 |
| 9 | 2.8024 | 2.9517 | 5.06 |
| 10 | 3.1217 | 3.2024 | 2.52 |

After isolated spectral rearrangements are excluded, the mean minimum stability margin factor over the working interval is 25.52, the median is 25.61, and the coefficient of variation is 0.899%. A persistent global minimum develops near $t$ = 79.13 s; its lowest original physical value is 25.11. Figure 4 additionally marks only those states for which independent analyses were performed.

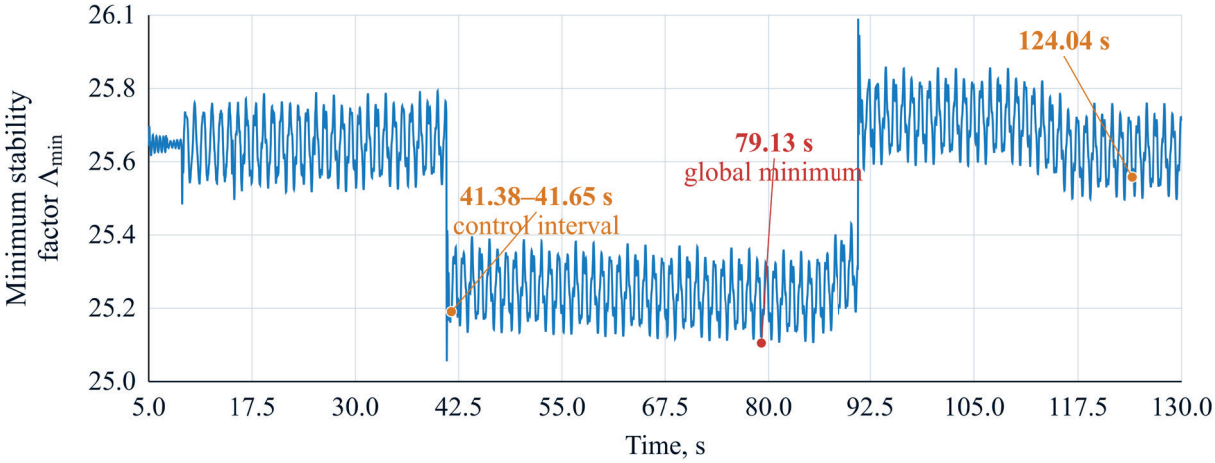



*Figure 4. Time history of the minimum stability factor and the investigated states*

### *4.2. Nonlinear Analyses of the Investigated States*

At $t$ = 41.38 s, the maximum translational displacement of the dynamic model is 69.994 mm and occurs at node 157. The nonlinear stability analysis yielded a critical load multiplier of 48.217358. After this maximum was reached, a stable descending equilibrium branch developed.

At $t$ = 79.13 s, the maximum translational displacement of node 157 is 71.317 mm, and the critical load multiplier is 44.429428. Thus, relative to the state at $t$ = 41.38 s, both the direct dynamic method and the nonlinear analysis indicate a reduction in the stability margin.

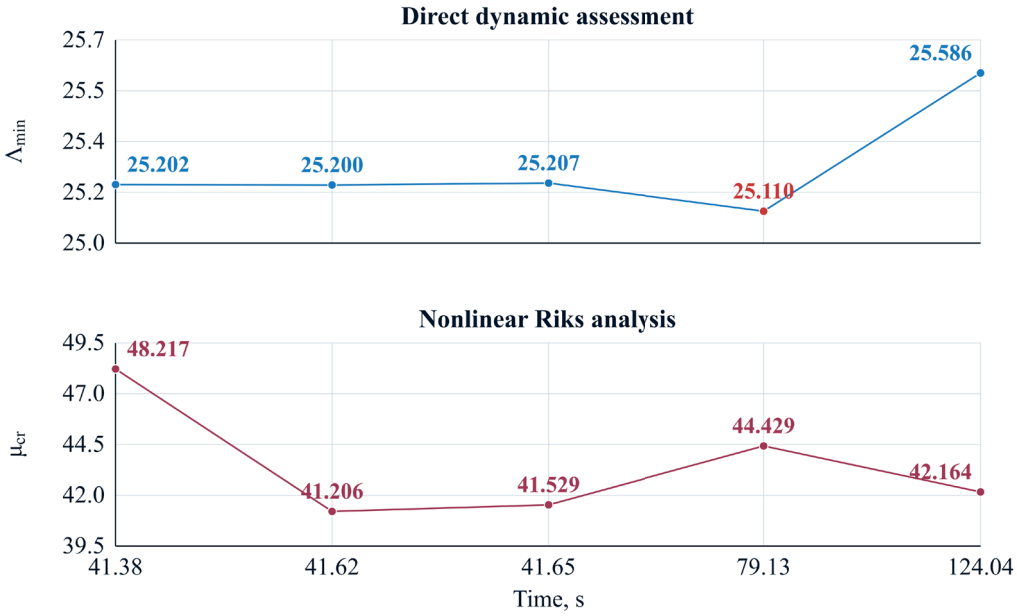



*Figure 5. Comparison of the direct and nonlinear stability assessments*

The extended series also includes the states at $t$ = 41.62 and 41.65 s, selected from displacement maxima at nodes 103 and 156. Their critical multipliers are 41.206482 and 41.529232, respectively. For the state at $t$ = 124.04 s, the completed analysis reached a critical multiplier of 42.164177 and continued onto a descending branch, ending at 42.103489.

Comparison of the two analyses in Figure 5 shows a mirror-like variation of the principal indicators $\Lambda_{min}$ (stability margin factor, SMF) and $\mu_{cr}$ (load proportionality factor, LPF).

Figures 6–10 show the complete equilibrium paths for the five investigated states. The abscissa gives the translational displacement of the corresponding control node, and the ordinate gives the current load multiplier. All five states, at $t$ = 41.38, 41.62, 41.65, 79.13 and 124.04 s, exhibit a maximum followed by a descending branch. For the state at 124.04 s, the completed calculation establishes the critical multiplier as 42.164177. Large post-critical displacements characterise numerical continuation of the path and are not interpreted as service displacements of the structure.

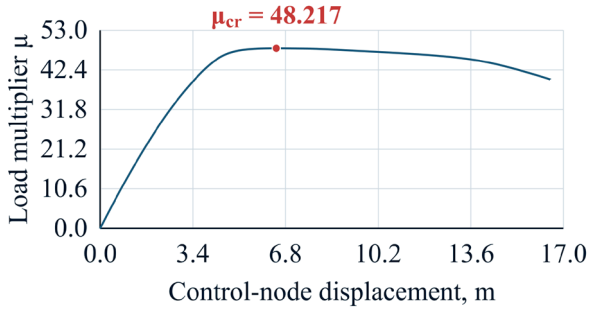



*Figure 6. Abaqus equilibrium path obtained by the Riks method at t = 41.38 s (control node 157)*

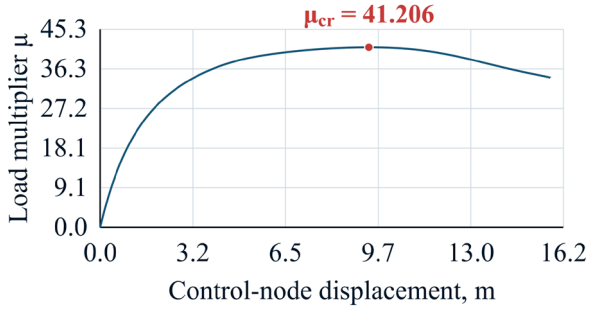



*Figure 7. Abaqus equilibrium path obtained by the Riks method at t = 41.62 s (control node 103)*

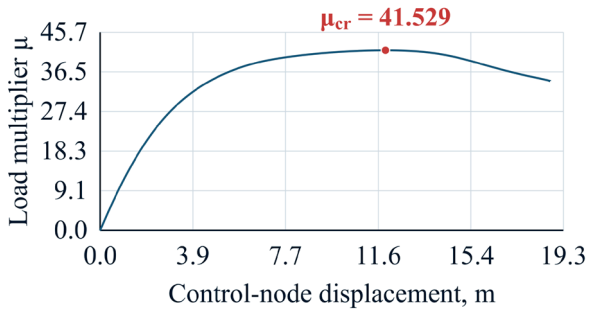



*Figure 8. Abaqus equilibrium path obtained by the Riks method at t = 41.65 s (control node 156)*

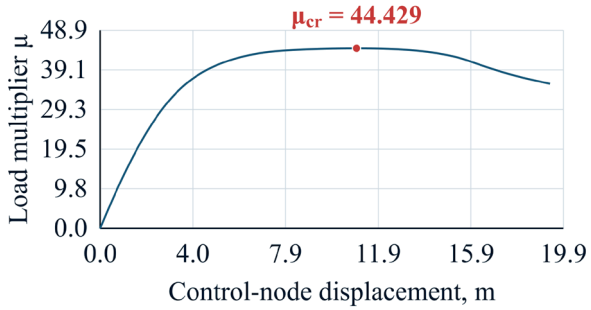



*Figure 9. Abaqus equilibrium path obtained by the Riks method at t = 79.13 s (control node 157)*

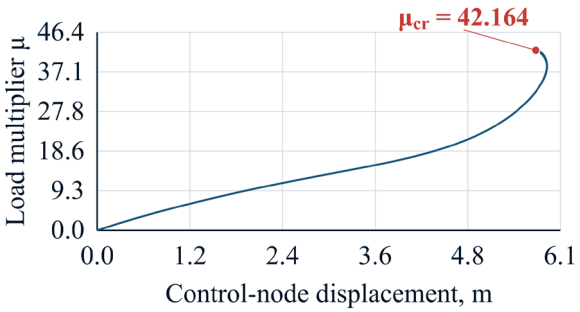



*Figure 10. Abaqus equilibrium path obtained by the Riks method at t = 124.04 s (control node 225)*

For the two strictly comparable time sections, both methods give the same ranking: the state at $t$ = 79.13 s is more unfavourable than that at $t$ = 41.38 s. The difference between the Python stability margin factors at the two instants is only 0.366%, whereas the corresponding difference in SIMULIA Abaqus is 8.526%. The LPF exceeds the directly calculated SMF by 91.32% at 41.38 s and by 76.94% at 79.13 s (Table 3).

*Table 3. Comparison of the direct and nonlinear stability assessments*

| t, s | Selection criterion | $\Lambda_{min}$ | $\mu_{cr}$ | $\mu_{cr}$ higher, % |
|---|---|---|---|---|
| 41.38 | Minimum associated with the multimodal response interval | 25.202190 | 48.217358 | 91.32 |
| 41.62 | Maximum displacement of node 103 | 25.246190 | 41.206482 | 63.22 |
| 41.65 | Maximum displacement of node 156 | 25.261070 | 41.529232 | 64.40 |
| 79.13 | Global minimum of $\Lambda_{min}$ | 25.109920 | 44.429428 | 76.94 |
| 124.04 | Maximum displacement of node 225 | 25.679420 | 42.164177 | 64.19 |

### *4.3. Time Sections Associated with Maximum Control-Node Displacements*

Quasi-static stability was assessed at time instants selected using a local kinematic criterion from the direct dynamic analysis in SIMULIA Abaqus. This analysis uses Rayleigh damping calibrated against the first and 111th natural frequencies. The extrema of the displacement components at nodes 103, 156 and 225 occur at $t$ = 41.62 s, approximately 41.65 s and 124.04 s, respectively.

At node 103, the maximum $U_1$ is 29.5477 mm; at node 156, the minimum $U_2$ is −69.9383 mm; and at node 225, the minimum $U_2$ is −115.8233 mm.

These states are identified from the single adopted dynamic solution in SIMULIA Abaqus and used as independent control points for quasi-static analysis.

Figure 11 presents fragments of the time histories around the three control extrema. Red points mark the extrema used to select the frozen states. The extrema at nodes 103 and 156 belong to the interval 41.62–41.65 s, whereas the extremum at node 225 occurs during the impulsive change in response at 124.04 s. None of these local kinematic points coincides with the global minimum stability margin factor at 79.13 s.

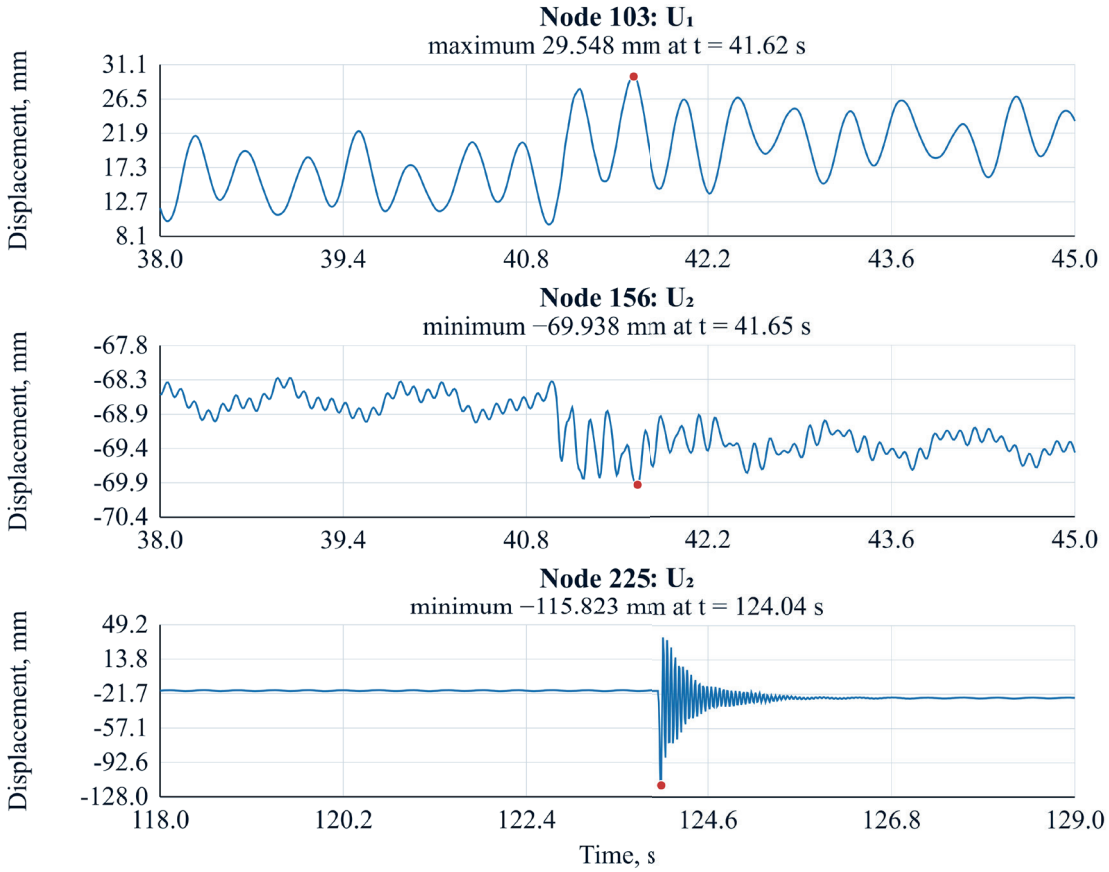



*Figure 11. Dynamic response of the Abaqus control nodes with Rayleigh damping calibrated against eigenmodes 1 and 111*

## 5. DISCUSSION

### *5.1. Interpretation of the Compared Criteria*

The proposed factor $\Lambda_{min}$ and the nonlinear critical multiplier $\mu_{cr}$ characterise different mathematical formulations. In the direct method, the inertia contribution simultaneously modifies the instantaneous eigenvalue operator and the local internal forces governing the geometric stiffness of the computational model. In the Riks method, the fixed loading of the selected state is increased proportionally. Their numerical values should therefore be compared in terms of trends and ranking, rather than treating one as a reference value for the other.

The principal comparison criteria are agreement in the unfavourable time interval, ranking of the investigated states and the pattern of change in the stability margin factor. The identical ranking at $t$ = 41.38 and 79.13 s confirms the ability of the proposed direct method to identify the more unfavourable state. Differences across the full series show that incorporating inertia into the instantaneous eigenvalue problem provides information absent from the frozen quasi-static formulation.

### *5.2. Selection of the Governing Instant*

The maximum displacement of an individual node characterises a local kinematic response, whereas $\Lambda_{min}$ is obtained by solving a global eigenvalue problem for the entire system. The states at $t$ = 41.62, 41.65 and 124.04 s are therefore useful independent control points, but do not replace the search for the minimum stability margin factor over the complete time history. The minimum at $t$ = 79.13 s was found without preselecting a control node.

The resulting series demonstrates the distinction between two ways of selecting an analysis state.

The displacement extrema at nodes 103 and 156 occur within the narrow interval 41.62–41.65 s, whereas the global dynamic minimum occurs substantially later. The proposed method thus extends conventional analysis: it does not discard local control indicators, but supplements them with a global criterion operating over the entire motion trajectory.

### *5.3. Numerical Robustness and Limitations*

Numerical stability of the instantaneous spectrum is an essential part of the direct method. Individual eigenvalues may briefly change order or switch between spectral branches. A physical minimum must therefore be confirmed over a sequence of neighbouring time samples and remain associated with the same eigenmode.

The limitations include linear material elasticity in the direct dynamic model implemented in Python and mixed kinematics for very short beam finite elements. The quasi-static Abaqus model does not include systematic variation of initial imperfections. The Python and Abaqus models use similar, but not identical, methods to form the local finite-element matrices.

Despite these limitations, comparison of the two approaches identifies two robust findings. First, the natural frequencies agree well between the independent models, while the control dynamic extrema in SIMULIA Abaqus provide additional states for nonlinear verification. Second, without preselecting a control node, the direct method identifies an unfavourable time interval and ranks the two principal global states consistently with the nonlinear analysis.

## CONCLUSION

- A consistent procedure for instantaneous stability assessment of a frame during time-domain dynamic analysis has been developed. It accounts for inertia forces on the left-hand side of the eigenvalue problem and all local internal-force components N–Q–M.
- Stability of the complete finite-element model of the industrial load-bearing structure, comprising 246 nodes and 369 finite elements, was analysed at 12,498 working time samples with a step of 0.01 s.
- In the adopted direct dynamic analysis in SIMULIA Abaqus, with damping calibrated against the first and 111$^{th}$ natural frequencies, the control extrema were $U_1$ = 29.5477 mm at node 103 at $t$ = 41.62 s, $U_2$ = −69.9383 mm at node 156 at $t$ = 41.65 s, and $U_2$ = −115.8233 mm at node 225 at $t$ = 124.04 s.
- The physical minimum of the first mode occurred at t = 79.13 s, with a stability margin factor $\mathbf{\Lambda}_{min}$ = 25.109920.
- The states at $t$ = 41.38, 41.62, 41.65, 79.13 and 124.04 s were investigated nonlinearly. The critical multipliers were 48.217, 41.206, 41.529, 44.429 and 42.164, respectively. A descending branch was obtained for each state.
- Both methods ranked the two consistently transferred states identically: $t$ = 79.13 s is more unfavourable than 41.38 s. The absolute minimum stability factors differ because of the different approaches to stability analysis and should not be compared as a result and a reference value.
- Selecting a time section solely from the maximum nodal displacement for the Riks method implemented in SIMULIA Abaqus is not a universal procedure.
- Automated identification of an unfavourable instant requires a robust criterion combining median filtering, temporal persistence of the minimum and eigenmode tracking.

*The work was supported by the Russian Science Foundation (project No. 25-11-00140).*

## REFERENCES

1. **Clough R.W.** The finite element method in plane stress analysis. // Proceedings of the 2nd ASCE Conference on Electronic Computation, Pittsburgh, 1960, pp. 345-378.
2. **Zienkiewicz O.C., Taylor R.L.** The Finite Element Method for Solid and Structural Mechanics. 6th ed. Oxford, Butterworth-Heinemann, 2005, 736 pages.

3. **Bathe K.J., Wilson E.L.** Numerical Methods in Finite Element Analysis. Englewood Cliffs, Prentice-Hall, 1976, 528 pages.
4. **Chen W.F., Lui E.M.** Structural Stability: Theory and Implementation. New York, Elsevier, 1987, 608 pages.
5. **EN 1993-1-1:2005.** Eurocode 3: Design of steel structures. Part 1-1: General rules and rules for buildings. Brussels, CEN, 2005, 90 pages.
6. **SP 16.13330.2017.** Steel Structures. Updated Edition of SNiP II-23-81*. Moscow, Standartinform, 2017, 104 pages. (in Russian).
7. **Bolotin V.V.** The Dynamic Stability of Elastic Systems. San Francisco, Holden-Day, 1964, 432 pages.
8. **Lyapunov A.M.** The General Problem of the Stability of Motion. Kharkov, Kharkov Mathematical Society, 1892, 250 pages. (in Russian).
9. **Alfutov N.A.** Fundamentals of the Theory of Stability of Deformable Systems. 2nd ed. Moscow, Mashinostroenie, 1995, 336 pages. (in Russian).
10. **Simitses G.J., Hodges D.H.** Fundamentals of Structural Stability. Burlington, Butterworth-Heinemann, 2006, 389 pages.
11. **Scanlan R.H.** The action of wind on suspension bridges. // Journal of Engineering Mechanics, Volume 117, No. 4, 1991, pp. 813-832. DOI: 10.1061/(ASCE)0733-9399(1991)117:4(813).
12. **Priestley M.J.N., Calvi G.M., Kowalsky M.J.** Displacement-Based Seismic Design of Structures. Pavia, IUSS Press, 2007, 720 pages.
13. **Timoshenko S.P., Gere J.M.** Mechanics of Materials. Moscow, Mir, 1976, 669 pages. (in Russian).
14. **Sidorov V.N., Badina E.S., Detina E.P.** Nonlocal in time model of material damping in composite structural elements dynamic analysis. // International Journal for Computational Civil and Structural Engineering, Volume 17, No. 4, 2021, pp. 14-21. DOI: 10.22337/2587-9618-2021-17-4-14-21.
15. **Sidorov V.N., Badina E.S., Klimushkin D.O.** Modification of the Rayleigh dissipation function for numerical modelling of internal damping in rod structures. // Vestnik MGSU, Volume 19, No. 6, 2024, pp. 960-970. (in Russian). DOI: 10.22227/1997-0935.2024.6.960-970.
16. **Alexandrov A.V., Potapov V.D., Zylev V.B.** Structural Mechanics. Book 2. Dynamics and Stability of Elastic Systems. Moscow, Vysshaya Shkola, 2008, 385 pages. (in Russian).
17. **Alfutov N.A., Kolesnikov K.S.** Stability of Motion and Equilibrium. Moscow, Bauman Moscow State Technical University Press, 2003, 255 pages. (in Russian).
18. **Sidorov V.N., Badina E.S.** The Finite Element Method in Stability and Vibration Problems of Rod Structures: Calculation Examples in Mathcad and MATLAB. Moscow, ASV Publishing House, 2021, 173 pages. (in Russian).
19. **Sidorov V.N., Klimushkin D.O.** Accounting for the complete deformation of rod structural elements in numerical stability analysis. // Proceedings of the International Conference, Saransk, National Research Mordovia State University, 2025, pp. 108-116. (in Russian). ISBN 978-5-7103-4933-5.
20. **Dassault Systèmes SIMULIA Corp.** Abaqus Analysis User's Manual. Version 2024. Providence, RI, Dassault Systèmes SIMULIA Corp., 2024.
21. **Crisfield M.A.** A fast incremental/iterative solution procedure that handles 'snap-through'. // Computers & Structures, Volume 13, No. 1-3, 1981, pp. 55-62. DOI: 10.1016/0045-7949(81)90108-5.

## СПИСОК ЛИТЕРАТУРЫ

1. **Clough R.W.** The finite element method in plane stress analysis. // Proceedings of the

2nd ASCE Conference on Electronic Computation, Pittsburgh, 1960, pp. 345-378.
2. **Zienkiewicz O.C., Taylor R.L.** The Finite Element Method for Solid and Structural Mechanics. 6th ed. Oxford, Butterworth-Heinemann, 2005, 736 pages.
3. **Bathe K.J., Wilson E.L.** Numerical Methods in Finite Element Analysis. Englewood Cliffs, Prentice-Hall, 1976, 528 pages.
4. **Chen W.F., Lui E.M.** Structural Stability: Theory and Implementation. New York, Elsevier, 1987, 608 pages.
5. **EN 1993-1-1:2005.** Eurocode 3: Design of steel structures. Part 1-1: General rules and rules for buildings. Brussels, CEN, 2005, 90 pages.
6. **СП 16.13330.2017.** Стальные конструкции. Актуализированная редакция СНиП II-23-81*. М., Стандартинформ, 2017, 104 с.
7. **Bolotin V.V.** The Dynamic Stability of Elastic Systems. San Francisco, Holden-Day, 1964, 432 pages.
8. **Ляпунов А.М.** Общая задача об устойчивости движения. Харьков, Харьковское математическое общество, 1892, 250 с.
9. **Алфутов Н.А.** Основы теории устойчивости деформируемых систем. 2-е изд. М., Машиностроение, 1995, 336 с.
10. **Simitses G.J., Hodges D.H.** Fundamentals of Structural Stability. Burlington, Butterworth-Heinemann, 2006, 389 pages.
11. **Scanlan R.H.** The action of wind on suspension bridges. // Journal of Engineering Mechanics, Volume 117, No. 4, 1991, pp. 813-832. DOI: 10.1061/(ASCE)0733-9399(1991)117:4(813).
12. **Priestley M.J.N., Calvi G.M., Kowalsky M.J.** Displacement-Based Seismic Design of Structures. Pavia, IUSS Press, 2007, 720 pages.
13. **Тимошенко С.П., Гере Дж.М.** Механика материалов. М., Мир, 1976, 669 с.
14. **Sidorov V.N., Badina E.S., Detina E.P.** Nonlocal in time model of material damping in composite structural elements dynamic analysis. // International Journal for Computational Civil and Structural Engineering, Volume 17, No. 4, 2021, pp. 14-21. DOI: 10.22337/2587-9618-2021-17-4-14-21.
15. **Сидоров В.Н., Бадьина Е.С., Климушкин Д.О.** Модификация функции диссипации Рэлея для численного моделирования внутреннего демпфирования в стержневых конструкциях. // Вестник МГСУ, Том 19, № 6, 2024, с. 960-970. DOI: 10.22227/1997-0935.2024.6.960-970.
16. **Александров А.В., Потапов В.Д., Зылев В.Б.** Строительная механика. Книга 2. Динамика и устойчивость упругих систем. М., Высшая школа, 2008, 385 с.
17. **Алфутов Н.А., Колесников К.С.** Устойчивость движения и равновесия. М., Издательство МГТУ им. Н.Э. Баумана, 2003, 255 с.
18. **Сидоров В.Н., Бадьина Е.С.** Метод конечных элементов в задачах устойчивости и колебаний стержневых конструкций. Примеры расчётов в Mathcad и MATLAB. М., Издательство АСВ, 2021, 173 с.
19. **Сидоров В.Н., Климушкин Д.О.** Учёт полного деформирования элементов стержневых конструкций при численном анализе устойчивости. // Материалы международной конференции, Саранск, МГУ им. Н.П. Огарёва, 2025, с. 108-116. ISBN 978-5-7103-4933-5.
20. **Dassault Systèmes SIMULIA Corp.** Abaqus Analysis User's Manual. Version 2024. Providence, RI, Dassault Systèmes SIMULIA Corp., 2024.
21. **Crisfield M.A.** A fast incremental/iterative solution procedure that handles 'snap-through'. // Computers & Structures, Volume 13, No. 1-3, 1981, pp. 55-62. DOI: 10.1016/0045-7949(81)90108-5.

*Vladimir Nikolaevich Sidorov* – Academician of Russian Academy of Architecture and Construction Science, Dr.Sc, Professor, Head of the Department of Computer Science and Applied Mathematics, National Research University Moscow State University of Civil Engineering, 129337, Russia, Moscow, Yaroslavskoye Shosse,b. 26, Professor of «Building Structures, Buildings and Facilities» Department, Institute of Railway Track, Construction and Structures, Russian University of Transport (MIIT), Professor of Department «Engineering Structures and Numerical Mechanics», Perm National Research Polytechnic University; ORCID: 0000-0001-8812-8022, e-mail: sidorov.vladimir@gmail.com.

*Vadim Kayumovich. Akhmetov,* Doctor of Science, Professor, Department of Computer Science and Applied Mathematics, Moscow State University of Civil Engineering, 26, Yaroslavskoe Shosse, Moscow, 129337, Russia, e-mail: vadim.akhmetov@gmail.com.

*Dmitriy Olegovich Klimushkin* – postgraduate student of the Department of Computer Science and Applied Mathematics, National Research University Moscow State University of Civil Engineering; 129337, Russia, Moscow, Yaroslavskoye Shosse,b. 26, e-mail:d.o.klimushkin@gmail.com

Contribution of the authors: all authors made equivalent contributions to the publication.
The authors declare that there is no conflict of interest.

*Владимир Николаевич Сидоров* — академик РААСН, доктор технических наук, профессор, заведующий кафедрой прикладной математики, Национальный исследовательский Московский государственный строительный университет, Ярославское шоссе, д. 26, Москва, 129337, Россия; ORCID: 0000-0001-8812-80221; e-mail: sidorov.vladimir@gmail.com

*Ахметов Вадим Каюмович,* доктор технических наук, профессор кафедры информатики и прикладной математики Национального исследовательского Московского государственного строительного университета, 129337, г. Москва, Ярославское шоссе, д. 26, e-mail: vadim.akhmetov@gmail.com

*Дмитрий Олегович Климушкин* – аспирант кафедры прикладной математики, Национальный исследовательский Московский государственный строительный университет, Ярославское шоссе, д. 26, Москва, 129337, Россия; ORCID: 0009-0007-7147-4595; e-mail: d.o.klimushkin@gmail.com

Вклад авторов: все авторы внесли равноценный вклад в подготовку публикации.
Авторы заявляют об отсутствии конфликта интересов